Journal Pre-proofs

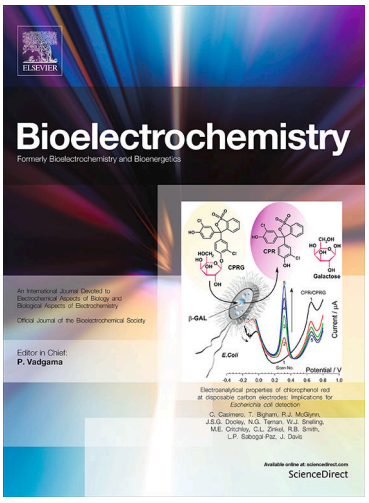

Ultra-sensitive and Selective Electrochemical Biosensor with Aptamer Recognition Surface Based on Polymer Quantum Dots and C_{60}/MWCNTs- Polyethylenimine Nanocomposites for analysis of Thrombin Protein

Hamid Reza Jamei, Behzad Rezaei, Ali Asghar Ensafi

PII: S1567-5394(20)30624-1
DOI: https://doi.org/10.1016/j.bioelechem.2020.107701
Reference: BIOJEC 107701

To appear in: *Bioelectrochemistry*

Received Date: 3 July 2020
Revised Date: 2 November 2020
Accepted Date: 5 November 2020

Please cite this article as: H. Reza Jamei, B. Rezaei, A. Asghar Ensafi, Ultra-sensitive and Selective Electrochemical Biosensor with Aptamer Recognition Surface Based on Polymer Quantum Dots and C_{60}/MWCNTs- Polyethylenimine Nanocomposites for analysis of Thrombin Protein, *Bioelectrochemistry* (2020), doi: https://doi.org/10.1016/j.bioelechem.2020.107701

Ultra-sensitive and Selective Electrochemical Biosensor with Aptamer Recognition Surface Based on Polymer Quantum Dots and C_{60}/MWCNTs-Polyethylenimine Nanocomposites for analysis of Thrombin Protein

Hamid Reza Jamei, Behzad Rezaei*[1], Ali Asghar Ensafi

Department of Chemistry, Isfahan University of Technology, Isfahan, 84156-83111 I.R. Iran

Abstract

In this study, an ultra-sensitive and selective Thrombin biosensor with aptamer-recognition surface is introduced based on carbon nanocomposite. To prepare the this biosensor, screen-printed carbon electrodes (SPCE) were modified with a nanocomposite made from fullerene (C_{60}), multi-walled carbon nanotubes (MWCNTs), polyethylenimine (PEI) and polymer quantum dots (PQdot). The unique characteristics of each component of the C_{60}/MWCNTs-PEI/PQdot nanocomposite allow for synergy between nanoparticles while polymer quantum dots resulted in characteristics such as high stability, high surface to volume ratio, high electrical conductivity, high biocompatibility, and high mechanical and chemical stability. The large number of amine groups in C_{60}/MWCNTs-PEI/PQdot nanocomposite created more sites for better covalent immobilization of amino-linked aptamer (APT) which improved the sensitivity and stability of the aptasensor. Differential Pulse Voltammetry (DPV) method with probe solution was used as the measurment method. Binding of thrombin protein to aptamers immobilized on the transducer resulted in reduced electron transfer at the electrode/electrolyte interface which reduces the peak

[1] Corresponding author. Tel: +983133913268, Fax: +983133912350

E-mail: rezaei@cc.iut. ac.ir

current (I_P) in DPV. The calibration curve was drawn using the changes in the peak current (ΔI_P),. The proposed aptasensor has a very low detection limit of 6 fmol L^{-1}, and a large linear range of 50 fmol L^{-1} to 20 nmol L^{-1}. Furthermore, the proposed C_{60}/MWCNTs-PEI/PQdot/APT aptasensor has good reproducibility, great selectivity, low response time and a good stability during its storage. Finally, the application of the proposed aptasensor for measuring thrombin on human blood serum samples was investigated. This aptasensor can be useful in bioengineering and biomedicine applications as well as for clinical studies.

Keywords: Thrombin; Aptamer; polymer Quantum dot; Fullerene; Multi-walled Carbon Nanotubes; Electrochemical aptasensor

1. Introduction

At the molecular level, all biomechanisms in cells are carried out through proteins, nucleic acids and interactions between them. The molecular basis of most diseases is a disorder or interference in normal activities of proteins active in cellular biomechanisms [1-3]. If proteins' activities diverge from their normal values, it can lead to various diseases including cancer [4]. Cancer is one of the largest predicted medical challenges and estimations have shown that by year 2030, more than 24 million people worldwide will be suffering from cancer [5]. Measuring and analysis of proteins in biological samples plays an important role in medical treatments, bioengineering, and nutritional safety and health applications [6]. One of the preferred methods for dealing with various conditions is their fast diagnosis through biomarkers and tumor-markers which plays an important role in proper treatment of these conditions [7]. Although various advancements have been reported in fast identification of proteins in biological samples, investigations are still ongoing for creating methods for fast and reliable detection of various proteins [8-10].

Thrombin or Factor II is one of the important proteins and biomarkers in humans which plays a central role in blood clot dissolution and tissue regeneration [11, 2]. This protein is used as a protein model in clinical studies and diagnoses and has a chain of 258 amino acids. Thrombin molecule has a length of 84 Å and a width of 34 Å, with a molecular weight of 28,400Da [6]. This protein is a Serine protease enzyme that turns soluble Fibrinogen to insoluble Fibrin [12]. Thrombin can also act as a hormone for Platelet aggregation, activation of endothelial cells and other important biological responses. Furthermore, in a healthy brain, thrombin is the regulator for duplication, differentiation and development of neurons [13,14]. Therefore, the development of thrombin sensors with high sensitivity and selectivity can play an important role in clinical diagnoses [15].

Today, characteristics and capabilities of aptamers (short single-stranded DNA/RNA molecules) have resulted in increased attention toward these molecules for biosensor manufacturing [16]. Along with high selectivity of aptamers for binding of an analyte, their unique characteristics have resulted in various advantages compared to other identifying biomolecules such as antibodies [17, 2]. These characteristics include small size compared to antibodies, high stability, structural stability during physical changes such as changes in pressure, temperature, pH, metal ions, etc. [18, 19], their ability for binding with a diverse set of targets from ions such as K^+ to cancer cells and microorganisms such as bacteria and viruses, the ability for various modifications with different chemical groups, easy immobilization on various surfaces, stability for long-term storage and easy transportation at ambient temperature, higher affinity binding and low dissociation rate as well as specific and selective binding [20]. On the other hand, the use of antibodies as biosensors comes with problems such as low stability, difficult manufacturing, limited storage time and irreversible temperature denaturing [21].

To this day, various aptamer-based biosensors have been reported for analysis of thrombin using methods including optical methods [22], quartz crystal microbalance (QCM) [23], field-effect transistors [24], fluorescence [25], surface-enhanced Raman scattering (SERS) [26], quartz microbalance crystal [27], surface plasmon resonance [28], colorimetric assay [29] and electrochemical methods [30-35]. However, the advantages of electrochemical aptasensors such as cheap manufacturing, simple structure, portability, the possibility for miniaturization, and high selectivity, have attracted various researchers to this type of aptasensors [36-39].

One of the most important steps in the manufacturing of an aptasensor is the covalent immobilization of aptamer on the transducer which has a direct effect on sensor stability and sensitivity [6, 40]. As a result, various nanomaterials are often used for development of aptasensors and better covalent immobilization of aptamers [41,42]. To this day, studies have reported the manufacturing of electrochemical aptasensors using various polyelectronic polymers, carbon nanomaterials such as multiwalled carbon nanotubes, graphene, carbon quantum dots as well as metal nanoparticles such as gold and silver nanoparticles [43-46].

One of the nanomaterials with significant use in manufacturing of electrochemical aptasensors is multi-walled carbon nanotubes (MWCNTs). Multi-walled carbon nanotubes offer characteristics such as suitable mechanical stability, high surface to volume ratio, inexpensive price, electrocatalytic characteristics, and biocompatibility, making them attractive for manufacturing of biosensors [46,47]. One of the other important carbon-based nanomaterials is fullerene (C_{60}) which has received a great deal of attention. Fullerene is one of the synthetic carbon morphologies which is created by heating graphite. Fullerene offers characteristics such as high chemical and mechanical stability, high surface to volume ratio, lack of metallic

impurities, electrocatalytic properties, high electronic conductivity, good biocompatibility and inert behavior [48,49].

Surface modification using conductive or non-conductive polymers is used to improve the adsorption of biological species on carbon-based materials [42, 46]. Carbon electrodes modified with polymers show significant improvements in selectivity, stability, and repeatability of electrode response for various analytics [9, 46]. PEI is one of the polymers which can be used as a stabilizing film on the surface of carbon-based materials. PEI offers advantages such as formation of thin films, biocompatibility, inexpensive price, low toxicity, ease of separation and recycling and odorless nature while presence of a large number of amine groups on its structure helps in better immobilization of biological compounds on electrochemical aptasensors [50-52]. polymer quantum dots are formed through agglomeration of polymer chains attached to a carbon core and are known as non-conjugated polymer quantum dots. Along with the advantages of carbon quantum dots, polymer quantum dots offer other advantages such as inert behavior and easy synthesis at room temperature [53-56].

In this study, for the first time, the characteristic of polymer quantum dots was used in the manufacturing of electrochemical aptasensors. To develop a sensitive thrombin aptasensor, C_{60}/MWCNTs-PEI/PQdot composite was used for the development of a biorecognition surface. Better aptamer covalent immobilization, increased sensitivity and higher stability due to the synergy between various nanomaterials in this nanocomposite resulted in a very sensitive and selective electrochemical aptasensor with high stability and repeatability. The proposed nanocomposite offers advantages such as high surface to volume ratio, high electrical conductivity, and presence of a large number of surface amine groups for better covalent immobilization of aptamer and high mechanical and chemical stability. In order to investigate the

performance of the proposed aptasensor, a recovery test was carried out in real human blood serum samples. The results indicated that the proposed aptasensor can be used as a suitable tool for biological and clinical studies for samples with complex matrices.

2. Experimental section

2.1. Chemicals and equipment

The amino-linked aptamer sequence used in the current study for analysis of thrombin protein was 5′-NH2- AGT CCG TGG TAG GGC AGG TTG GGG TGA CT-3" [57] which was acquired from Bioneer Co., South Korea. 1-ethyl-3-(3-di-methylaminopropyl) carbodiimide hydrochloride (EDC), glutaraldehyde (GLA), N-hydroxysuccinimide (NHS), diethylenetriamine (DETA, 99%), nitric acid (65%), MWCNTs (with a length of 5–9 μm bundles and a diameter of 50 – 100 nm), polyethyleneimine (PEI), L-ascorbic acid (99%) and fullerene-C_{60} (99.5%), human plasma thrombin, chicken egg white lysozyme (Lys), bovine hemoglobin (BHb), human IgG (IgG) and bovine serum albumin (BSA) were obtained from Sigma-Aldrich and Merck Company. All other equipment, instruments, and chemicals used in this study are fully explained in section 1 of the supplementary materials file.

2.2. Preparation of C_{60}/MWCNTs-PEI

To prepare C_{60}/MWCNTs-PEI, C_{60} was separately carboxylated. The Bingle - Hirsch reaction was used for the preparation of $C_{60}((COOH)_2)_n$ while MWCNTs were carboxylated through oxidation with nitric acid [58, 59]. Details of synthesis and characterization of $C_{60}((COOH)_2)_n$ and MWCNTs-COOH are presented in section 2 of the supplementary materials (figure S-1) and schematically presented in figure 1.

In order to prepare C_{60}/MWCNTs-PEI, first, 15.0 mg of $C_{60}((COOH)_2)_n$ and MWCNTs mixture with the 1:2 ratio was dispersed in 50.0 mL methanol before sonicating for 45 minutes in an ultrasound bath to create a fully homogeneous C_{60}/MWCNTs suspension. Then, 100.0 mg of 1-ethyl-3-(3-dimethylaminopropyl) carbodiimide hydrochloride (EDC) and 100.0 mg N-hydroxysuccinimide (NHS) were added to the suspension and the mixture was stirred slowly at room temperature for 3 h. Then, 100.0 mg of polyethylenimine (PEI) was added to the suspension before being stirred for 24 h at room temperature [51]. Finally, the resulting C_{60}/MWCNTs-PEI were washed several times with methanol and distilled water to remove any extra polymers, separated using a centrifuge and dried under vacuum. The schematic presented in figure 1 shows the synthesis method for C_{60}/MWCNTs-PEI.

2.3. Synthesis of Polymer Quantum dots

To synthesize the polymer quantum dots, the single-step method reported by Xia et.al. (2017) was used. Briefly, to synthesize polymer quantum dots, the first 2 mL of 0.50 M L^{-1} ascorbic acid solution was mixed with 1100 μL of 1.0 M diethylenetriamine (DETA) in a 25.0 mL volumetric flask and was brought to volume using double distilled water [54]. Then, the solution was sonicated for 20 minutes before being transfer to a 50.0 mL flask and stirring for 72 h at room temperature until its color changed from transparent to light yellow and finally to yellow (schematic 1). Finally, a 0.22 μm syringe filter and 30000 MWCO centrifuge filter were used to remove any impurities.

2.4. Preparation of C_{60}/MWCNTs-PEI/PQdot

In this stage, after the preparation of C_{60}/MWCNTs-PEI and PQdot, a suspension of C_{60}/MWCNTs-PEI/PQdot nanocomposite was prepared. First, 5.0 mg of C_{60}/MWCNTs-PEI was

added to 5.0 mL of ultrapure water and sonicated in an ultrasound bath for 1 h to fully disperse the solid. Then, 1000 µL of synthesized PQdots (with negative surface charge) was added to the C_{60}/MWCNTs-PEI suspension (which has a positive surface charge) and sonicated for one hour, resulting in a homogeneous suspension of C_{60}/MWCNTs-PEI/PQdot nanocomposite.

2.5. Preparation of biorecognition surface on the C60/MWCNTs-PEI/PQdot base

In this step, first, the surface of SPCE electrodes were electrochemically treated to clean and activate thier surface. For electrochemical pretreatment, 100µL of 0.5 M sulfuric acid solution and 0.1 M KCl solution was dropped on the surface of the electrodes before applying 15 cyclic voltammetry cycles in the range of 1.0 to -1.5 V with the scanning speed of 200 mV s^{-1}. Then, the electrodes surface was washed with ultrapure water and dried at room temperature before dropping 7 µL of C_{60}/MWCNTs-PEI/PQdot suspension on the surface of the electrodes and placing them in a clean environment for 2 h until fully dried. Then, glutaraldehyde (GLA) linker was used to attach covalently bonded amine groups to modified C_{60}/MWCNTs-PEI/PQdot electrodes. Afterward, 50µL of 5 vol% GLA solution was dropped on the surface of SPCE/C_{60}/MWCNTS-PEI/PQdot and the linker was allowed to react with SPCE/C_{60}/MWCNTs-PEI/PQdot surface for 60 minutes. Then, 50µL of aminated Thrombin aptamer with a concentration of 400 nM was dropped on the surface of SPCE/C_{60}/MWCNTs-PEI/PQdot/GLA electrode and the electrodes were placed in a humid room under refrigeration for 5 h until Thrombin aptamer created a thin covalently-bound film on the electrodes surface. The schematic of aptamer covalent immobilization process is presented in figure 1. The electrodes were then washed with ultrapure water to remove aptamers attached to the surface through non-covalent bonds. Then, to block the surface and reduce non-specific adsorption of molecules to the aptasensor surface and increased selectivity, 2% solution of bovine serum albumin (BSA) was

used. To this end, 50 µL of 2% BSA was dropped on the surface of SPCE/C_{60}/MWCNTs-PEI/PQdot/GLA/APT electrode and the surface of aptasensor was washed after one hour with ultrapure water. Electrochemical aptasensors were kept under refrigeration and were placed at room temperature 1 h before each experiment.

"Here Fig. 1"

2.6. Electrochemical measurements

In this study, Cyclic voltammetry (CV), Differential Pulse Voltammetry (DPV) and Electrochemical impedance spectroscopy (EIS) were used to investigate surface modification stages and aptasensor manufacturing as well as Thrombin analysis. The electrode used in this study was an screen-printed carbon electrodes (SPCE, model DRP-110) which is working electrode (4mm) made of Carbon. The counter electrode and reference electrode used in experiments were carbon and Ag electrodes, respectively. The electrolyte used in all tests was 2.5 mmol L^{-1} $[Fe(CN)_6]^{3-/4-}$ (1:1) solution as a redox probe and 0.1 mol L^{-1} KCl in Tris buffer (pH=7.4) and in all measurements 100 µL of this solution was dropped on SPCE surface.

The electrochemical impedance spectroscopy was conducted under constant conditions with a sinusoidal signal of 10 mV and a range of 100 mHz to 100 kHz, frequency potential applied of +0.13 V. In this method for impedance measurement was used a three electrode electrochemical cell. Using Z-view software and fitting the date acquired from EIS, the equivalent electrical circuit was determined (figure S-2 in supplementary materials, section 3). The DPV parameters included modulation amplitude of 50.0 mV, step potential of 8.0 mV, modulation time of 0.05 s, and interval time of 0.5 s. Cyclic voltammetry tests were carried out under constant conditions with a potential scanning between -0.2 and 0.6 V at a scan rate of 100 mV s^{-1}. All

electrochemical tests (EIS, DPV and CV) were carried out at room temperature using Ivuim potentio-galvanostat equipment (Model: Vertex) and using Ivium software.

3. Results and discussion

3.1. Characterization of Polymer Quantum dots

In this section, DLS, XRD, TEM, UV-vis-NIR and fluorescence spectroscopy techniques, FT-IR and zeta potential were used to determine successful synthesis of polymer quantum dots from L-Ascorbic acid and diethylenetriamine. The detailed results of these studies are presented in section 4 of the supplementary materials (Fig. S-3).

3.2. Surface Morphology of Nanocomposites

FE-SEM and TEM techniques were used to investigate the nanoscale morphology of electrodes surface after modification with different nanoparticles and nanocomposites. These results are presented in figure 2. Figure 2A shows the FE-SEM image of the bare SPCE electrode after electrochemical pretreatment and before any modification while figures 2B and 2C show the FE-SEM and TEM images of MWCNTs used in this study which clearly shows the nanotubes.

Figure 2D shows the TEM image of C_{60} used in this study while figure 2E shows the TEM images of C_{60}/MWCNTs with C_{60} deposited on the surface of MWCNTs, increasing its surface to volume ratio compared to bare MWCNTs. Figures 2F and 2G show the FE-SEM and TEM images of C_{60}/MWCNTs-PEI nanocomposite, both of which show the PEI polymer coated on the surface of C_{60}/MWCNTs nanocomposite.

Finally, figure 2H shows the TEM image of C_{60}/MWCNTs-PEI/PQdot, where polymer quantum dots with negative surface charges are electrostatically deposited on the surface of C_{60}/MWCNTs-PEI nanocomposite which has a positive charge. These images indicated successful manufacturing of nanocomposites and their use for uniform modification of electrodes surface.

3.3. EIS, DPV and CV investigation of electrodes modified with different nanocomposites

In this section, in order to investigate the amplifying role of modifiers, the signals for a 2.5 mmol L^{-1} $[Fe(CN)_6]^{3-/4-}$ (1:1) solution on the surface of bare SPCE electrode as well as electrodes modified with MWCNTs, C_{60}/MWCNTs, C_{60}/MWCNTs-PEI, and C60/MWCNTs-PEI/PQdot were measued using three techniques of cyclic voltammetry, differential pulse voltammetry and electrochemical impedance spectroscopy (figure 2I-K). In CV studies, the potential range of -0.2 to +0.6V versus reference electrode and a scan rate of 100mVs^{-1} were used and oxidation and reduction peaks of Ferro/Ferricyanide probe were recorded under various conditions. Figure 2J shows the DPV voltammograms which confirm CV results (figure 2I).

As it can be seen in figures 2I and 2J, the current resulting from oxidation and reduction of Ferro/Ferricyanide probe on the surface of SPCE electrode (trace a) modified with various nanomaterials is higher than the current for bare SPCE electrode. The significant increase in current is due to increased synergy between carbon nanoparticles used in modifier nanocomposites. MWCNTs and C_{60} result in improved electron transfer and increased peak current due to high surface to volume ratio and high electrical conductivity (trace b and c) [6,8, 48,49], while presence of PEI resulted in a relative increase in signal compared to C_{60}/MWCNTs due to presence of amine groups as well as facilitating the homogeneously of the nanomaterial suspension and better covalent immobilization of nanocomposites on electrodes surface (trace d).

The presence of polymer quantum dots on C_{60}/MWCNTs-PEI/PQdot resulted in a slight decrease in signal compared to the electrode modified with C_{60}/MWCNTs-PEI which is due to semiconductor characteristics of synthesized polymer quantum dots (trace e). To better evaluate the results regarding the development of electrodes surfaces, electrochemical impedance spectroscopy (EIS) was used. In this part, EIS related to the reversible reaction of potassium hexacyanoferrate on modified electrodes with various nanocomposites was investigated.

As it can be seen in figure 2K, the Nyquist curve confirms the charge transfer resistance for electrodes modified with various nanocomposites measured through DPV and CV results. Charge transfer resistance (R_{CT}) significantly decreased after using carbon-based modifiers with high electrical conductivity as well as PEI compared to the bare SPCE electrode. On the other hand, R_{CT} increased slightly in SPCE/C_{60}/MWCNTs-PEI/PQdot compared to SPCE/C_{60}/MWCNTs-PEI which is due to semi-conductive nature of polymer quantum dots. The Nyquist curves resulting from EIS were fitted with the help of Z-View software and its equivalent electrical circuit was determined (Fig. S-2).

"Here Fig. 2"

3.4. Optimization of parameters in aptasensor preparation

In this section, all factors affecting the manufacturing and response of Thrombin electrochemical aptasensor were optimized one factor at a time (The analyzes were repeated four times, n=4). The optimized parameters included aptamer concentration, aptamer covalent immobilization time and duration of interaction with thrombin. The optimization results, as well as details of the optimization, are presented in figure S-4 and section 5 of the supplementary materials file. The optimized values for aptamer concentration, aptamer covalent immobilization

time and duration of interaction with analyte were 400 nM, 5 and 1 h, respectively which were used for all future aptasensor manufacturing and measurements (Fig. S-4).

3.5. Comparison of different nanocomposites for aptamer covalent immobilization and measurement of thrombin

In this section, the covalent immobilization of aptamer on the surface of SPCE/C_{60}/MWCNTs, SPCE/C_{60}/MWCNTs-PEI and SPCE/C_{60}/MWCNTs-PEI/PQdot modified electrodes was investigated. Then, the analytical signal for each modified electrode in the presence of 0.005nM of thrombin was followed using DPV technique and under similar conditions using the Ferro/Ferricyanide probe signal. Figure 3A-F (The analyzes were repeated four times, n=4) show the voltammograms obtained from DPV techniques for SPCE/C_{60}/MWCNTs, SPCE/C_{60}/MWCNTs–PEI and SPCE/C_{60}/MWCNTs–PEI/PQdot modified electrodes in case of a bare electrode (trace a), after modification (trace b), after aptamer covalent immobilization and blocking the surface with BSA (trace c) and finally after interaction of aptasensor with a constant concentration of thrombin (trace d).

Manufacturing of thrombin aptasensor using various electrode modifications was carried out under optimum conditions stated above. Then, the current before and after aptamer covalent immobilization ($\Delta I_{Immobilization} = I_{Modified} - I_{Aptamer}$) was investigated for each electrode. Furthermore, peak current before and after binding of thrombin on the immobilized aptamers for different modifications ($\Delta I_{P(0.005nM)} = I_{aptamer} - I_{Thrombin}$) was used to determine sensitivity in the presence of thrombin (0.005nM). The results indicated that changes in current due to aptamer covalent immobilization ($\Delta I_{Immobilization}$) and interaction with thrombin ($\Delta I_{P(0.005nM)}$) under similar conditions are equal to $\Delta I_{Immobilization} = 1.9$, 6.1 and 12.2 μA and $\Delta I_{P(0.005nM)} = 2.7$, 5.3 and 14.9 μA for SPCE-C_{60}/MWCNTs, SPCE/C_{60}/MWCNTs-PEI and SPCE/C_{60}/MWCNTs-PEI/PQdot

aptasensors, respectively (figures 3B, 3D and 3F). These results indicated that SPCE-C_{60}/MWCNTs-PEI/PQdot has the highest aptamer immobilization current ($\Delta I_{Immobilization}$= 12.2μA) which is due to the presence of amine groups of polymer quantum dots and C_{60}/MWCNTs-PEI. Furthermore, the largest response to 0.005 nM of thrombin was also observed in this modified electrode ($\Delta I_{P(0.005nM)}$ =14.9 μA). These results indicate that the existence of polymer quantum dots in C_{60}/MWCNTs-PEI/PQdot decrease in signal ($I_{modified}$) due to their semiconductive behavior but the increase in surface and aptamer Immobilization sites can play an important role in improving aptamer immobilization and increased sensitivity of aptasensor.

Furthermore, in this part, aptamer immobilization through formation of covalent bonds between carboxyl groups of the nanocomposite on the base and amine groups of the aptamer using EDC and NHS was investigated. The results indicated that under similar conditions (immobilication duration and aptamer concnetraiton), the immoblilzation of apatamers using aptamer amine groups and carboxyl groups of C_{60}/MWCNTs nanocomposite and PQDot in $\Delta I_{Immobilization}$ of 4.9 and 3.4, respectively.

As shown in figure 3, the results indicate that using of C60/MWCNTs-PEI/PQdot nanocomposite provide a suitable base for a biorecognition surface, especially for electrochemical aptasensors.

"Here Fig. 3"

3.6. Thrombin detection

The calibration curve for electrochemical measurement of thrombin using SPCE/C_{60}/MWCNTs-PEI/PQdot/GLA/APT aptasensor was drawn by following the signal for

2.5 mmol L^{-1} $[Fe(CN)_6]^{3-/4-}$ (1:1) solution as a redox probe and 0.1 mol L^{-1} KCl in Tris buffer (pH = 7.4) using DPV technique. Then, several solutions with varying concentrations of thrombin were created in Tris buffer (pH = 7.4) and the current before and after interaction of SPCE/C_{60}/MWCNTs-PEI/PQdot/GLA/APT aptasensor with different concentration of thrombin was measured (n=3). The voltammogram results are presented in figure 4A. The binding of thrombin with immobilized aptamer in SPCE/C60/MWCNTs-PEI/PQdot/GLA/APT aptasensor creates a barrier for electron transfer in intersection of electrode and electrolyte, which means that increase in thrombin concentration follow with peak current decreases (figure 4A). The graph presented in figure 4B shows the changes in peak current ΔI_P versus changes in thrombin concentration. As can be seen, this calibration curve is nonlinear. Then, changes in peak current were drawn versus the logarithm of changes in thrombin concentration which resulted in a linear calibration curve (figure 4C). The calibration curve obtained for the proposed electrochemical aptasensor has a large linear dynamic range from 0.00005 nM to 20 nM and a detection limit of 6 fmol L^{-1} (at S/N ratio = 3).

Then, the results of SPCE/C_{60}/MWCNTs-PEI/PQdot/GLA/APT aptasensor were compared to the results of other electrochemical thrombin aptasensors introduced in recent years (table 1). As can be seen, the proposed aptasensor has a significantly lower detection limit and a larger than linear range compared to other electrochemical aptasensors. These results indicate that the proposed electrochemical aptasensor can be a powerful tool for clinical studies on proteins and biomarkers.

"Here Fig. 4 and Table 1"

3.7. Selectivity of aptasensor

Due to complex matrices of biological samples, selectivity of sensors to specific analytes is one of their most important features. In this section, the selectivity of SPCE/C_{60}/MWCNTs-PEI/PQdot/GLA/APT aptasensor in the presence of several proteins from the same family as thrombin was investigated. These proteins included bovine serum albumin (BSA), human IgG (IgG), lysozyme (Lys), and bovine hemoglobin (BHb). To this end, the proposed aptasensor was used to follow ΔI_P of thrombin using DPV technique in the presence of these proteins. The aptasensor response to thrombin (0.0005 nM) in a solution with BSA (0.05 nmol L^{-1}), IgG (0.05 nmol L^{-1}), Lys (0.01 nmol L^{-1}) and BHb (0.03 nmol L^{-1}) (n=4) is shown in figure 4D. As can be seen, the aptasensor response to thrombin is selective and shows good specificity even in presence of significantly higher concentrations of other proteins.

Then, the response of SPCE/C_{60}/MWCNTs-PEI/PQdot/GLA/APT aptasensor was investigated in the presence of each of the abovementioned proteins, separately. Figure S-5 shows high selectivity in aptasensor response and indicates that it can be used in complex biological matrices (section 6 of supplementary materials file).

3.8. Reproducibility and storage stability of proposed aptasensor

Another important parameter investigated in this study was the precision or reproducibility of aptasensor response. Accordingly, 10 different SPCE/C_{60}/MWCNTs-PEI/PQdot/GLA/APT aptasensors were manufactured in parallel under similar conditions and the ΔI_p signal for 0.0005nM of thrombin was followed for each aptasensor using DPV technique with the results presented in Table S-1. Then, the RSD value for the responses was calculated which was equal to 3.6%, indicating a good precision of the proposed aptasensor. The detailed results are presented in Table S-1 and section 7 of the supplementary materials file.

To investigate the storage stability of the proposed aptasensor, after preparation of SPCE/C_{60}/MWCNTs-PEI/PQdot/GLA/APT, the signal for 2.5 mmol L^{-1} $[Fe(CN)_6]^{3-/4-}$ (1:1) solution was measured using DPV in 30 consecutive days. Between measurements, the aptasensor was placed in dark environment at refrigerator and before each measurement was placed 1 hour at room temperature. The percentage change in aptasensor response compared to the response on the first day is shown in figure S-6. As can be seen in figure S-6, after 30 days, the aptasensor response showed only 15% decrease compare to the first day which indicates good storage stability of the aptasensor.

3.9. Application of aptasensor for thrombin detection in real samples

The application of the proposed aptasensor for thrombin detection was investigated using DPV and in real human blood serum samples. In this regard, three healthy human blood serum samples were prepared from the Medical Center of Isfahan University of Technology. Blood serum samples were perpraied from two men, 23 and 34 years old, and a woman, 28 years old. All ethical protocols were observed in the process of preparing blood serum samples from this center. The human serum samples were obtained from fresh blood samples by centrifuging (1000 rpm) for 5 minutes. The samples were diluted to $1/20^{th}$ of their original concentration using Tris buffer (pH=7.4). None of the samples showed any thrombin protein. Then, the recovery method was used by spiking each sample with three different volumes of standard thrombin samples with concentrations of 0.5, 5.0 and 50.0 pM and carrying out a recovery test. These results are presented in Table 2. The recovery percentage for these samples was between 95.4% and 104.2%. These results indicated that the proposed aptasensor can be used for measuring thrombin in real biological samples.

“Here Table 2”

4. Conclusion

In this study, a novel SPCE/C_{60}/MWCNTs-PEI/PQdot/GLA/APT aptasensor was developed for the analysis of thrombin protein. The C_{60}/MWCNTs-PEI/PQdot nanocomposites were used to modify the surface of SPCE electrode in order to manufacture a sensitive electrochemical aptasensor. These C_{60}/MWCNTs-PEI/PQdot nanocomposites offer unique characteristics such as high electrical conductivity, fast electron transfer kinetics, high surface to volume ratio, suitable stability and a high number of surface amine groups. The presence of high number of surface amine groups and high surface to volume ratio in this nanocomposite increased the number of available sites for thrombin binding. The use of polymer quantum dots for the development of electrochemical aptasensor for the first time showed that the unique characteristics and easy synthesis of these quantum dots and make them ideal for sensitive aptasensors.

Binding of thrombin on the surface of SPCE/C_{60}/MWCNTs-PEI/PQdot/GLA/APT aptasensor creates a barrier for electrons and restricts electron transfer in the interface between electrode and electrolyte (Ferro/Ferricyanide probe). This results in decrease in peak current in the presence of thrombin, providing an analytical signal dependent on thrombin concentration. Then, the detection limit and linear range of the proposed aptasensor were investigated and compared to other aptasensors. The results indicated that the proposed aptasensor has a lower detection limit and a larger linear range compared to similar aptasensors. Furthermore, reproducibility and storage stability of the proposed aptasensor was investigated and the results indicated high reproducibility for the proposed aptasensor. The proposed aptasensor was also

used in measurements in real samples and the results indicated that it can be used for measurements in complex biological matrices.

The proposed SPCE/C_{60}/MWCNTs-PEI/PQdot/GLA/APT aptasensor offers advantages compared to other similar thrombin electrochemical aptasensors including higher sensitivity and selectivity and can be used as a powerful tool in clinical and biological studies. Furthermore, unique characteristics of C_{60}/MWCNTs-PEI/PQdot as a powerful surface modifier can be used for the development of other similar biosensors.

Acknowledgments

The authors would like to thank the Research Council of Isfahan University of Technology, (IUT), the Iranian Nanotechnology Initiative Council and Center of Excellence in Sensor and Green Chemistry for their support and cooperation in this study.

Conflict of interest

Hamid Reza Jamei, Behzad Rezaei, Ali Asghar Ensafi declare that they have no conflict of interest.

Ethical approval

All procedures performed in studies involving human samples were in accordance with the ethical standards of the institutional and committee Isfahan University of Technology and with its later amendments or comparable ethical standards.

Permissions

The management of the Health Center of Isfahan University of Technology has authorized the use of blood samples in this study, and the publication of the results of the study of the mentioned samples has no conflict of interest.

Appendix A. Supplementary materials

Supplementary materials associated with this paper can be found in the "Supplementary materials" file.

References

[1] A.J. Barr, The biochemical basis of disease, Essays Biochem 62 (2018) 619-642. https://doi.org/10.1042/EBC20170054

[2] Y.X. Chen, K.J. Huang, L.L. He, Y.H. Wang, Tetrahedral DNA probe coupling with hybridization chain reaction for competitive thrombin aptasensor, Biosens. Bioelectron. 100 (2018) 274-281. https://doi.org/10.1016/j.bios.2017.09.022

[3] E. Reynaud, Protein misfolding and degenerative diseases, Nature Education 3 (2010) 28.

[4] Y. Liu, Z. Zhang, J. Wang, C. Chen, X. Tang, J. Zhu, J. Liu, Metabolic reprogramming results in abnormal glycolysis in gastric cancer, OncoTargets Ther. 12 (2019) 1195. https://doi.org/10.2147/OTT.S189687

[5] B.W. Stewart, C.P. Wild, World Cancer Report 2014, International Agency for Research on Cancer, Lyon, France, 2014, p. 89–99.

[6] E. Heydari-Bafrooei, M. Amini, M.H. Ardakani, An electrochemical aptasensor based on TiO2/MWCNT and a novel synthesized Schiff base nanocomposite for the ultrasensitive detection of thrombin, Biosens. Bioelectron. 85 (2016) 828-836. https://doi.org/10.1016/j.bios.2016.06.012

[7] L. Hui, L. Rixv, Z. Xiuying, A system for tumor heterogeneity evaluation and diagnosis based on tumor markers measured routinely in the laboratory, *Clin. Biochem*. *48* (2015) 1241-1245. https://doi.org/10.1016/j.clinbiochem.2015.07.027

[8] E. Heydari-Bafrooei, N.S. Shamszadeh, Electrochemical bioassay development for ultrasensitive aptasensing of prostate specific antigen, Biosens. Bioelectron. 91 (2017) 284-292. https://doi.org/10.1016/j.bios.2016.12.048

[9] B. Rezaei, H.R. Jamei, A.A. Ensafi, An ultrasensitive and selective electrochemical aptasensor based on rGO-MWCNTs/Chitosan/carbon quantum dot for the detection of lysozyme, Biosens. Bioelectron. 115 (2018) 37-44. https://doi.org/10.1016/j.bios.2018.05.012

[10] Z. Wei, X. Cai, J. Zhang, J. Fan, J. Xu, L. Xu, High Sensitive Immunoelectrochemical Measurement of Lung Cancer Tumor Marker ProGRP Based on TiO_2-Au Nanocomposite, Molecules 24 (2019) 656. https://doi.org/10.3390/molecules24040656

[11] V. Tutwiler, A.D. Peshkova, G. Le Minh, S. Zaitsev, R.I. Litvinov, D.B. Cines, J.W. Weisel, Blood clot contraction differentially modulates internal and external fibrinolysis, J. Thromb. Haemost. 17 (2019) 361-370. https://doi.org/10.1111/jth.14370

[12] ME. Maragoudakis, NE. Tsopanoglou, P. Andriopoulou, Mechanism of thrombin-induced angiogenesis, Biochem. Soc. Trans. 30 (2002) 173–177. https://doi.org/10.1042/bst0300173

[13] G. Xi, R.F. Keep, Y. Hua, J. Xiang, J.T. Hoff, Attenuation of thrombin-induced brain edema by cerebral thrombin preconditioning, Stroke 30 (1999) 1247-1254.

[14] T. Rohatgi, F. Sedehizade, K.G. Reymann, G. Reiser, Protease-activated receptors in neuronal development, neurodegeneration, and neuroprotection: thrombin as signaling molecule in the brain, Neuroscientist 10 (2004) 501-512. https://doi.org/10.1177/1073858404269955

[15] M. L. Nierodzik, S. Karpatkin, Thrombin induces tumor growth, metastasis, and angiogenesis: Evidence for a thrombin-regulated dormant tumor phenotype, Cancer Cell 10 (2006) 355-362. https://doi.org/10.1016/j.ccr.2006.10.002

[16] S.R. Yan, M.M. Foroughi, M. Safaei, S. Jahani, N. Ebrahimpoor, F. Borhani, N.R.Z. Baravati, Z Aramesh-Boroujeni, L.K. Foong, A Review: Recent advances in ultrasensitive and highly specific recognition aptasensors with various detection strategies, Int. J. Biol. Macromol.155 (2020) 184-207. https://doi.org/10.1016/j.ijbiomac.2020.03.173

[17] Y.N. Hou, J.F. Liu, M. Hong, X. Li, Y.H. Ma, Q.L. Yue, C.Z. Li, A reusable aptasensor of thrombin based on DNA machine employing resonance light scattering technique, Biosens. Bioelectron. 92 (2017) 259–265. https://doi.org/10.1016/j.bios.2017.02.024

[18] S.D. Jayasena, Aptamers: an emerging class of molecules that rival antibodies in diagnostics, Clin. Chem. 45 (1999) 1628-1650. https://doi.org/10.1093/clinchem/45.9.1628

[19] J.D. Munzar, A. Ng, D. Juncker, Duplexed aptamers: history, design, theory, and application to biosensing, Chem. Soc. Rev. 48 (2019) 1390-1419. https://doi.org/10.1039/C8CS00880A

[20] G.A. Zelada-Guillen, J. Riu, A. Duzgun, F.X. Rius, Immediate detection of living bacteria at ultralow concentrations using a carbon nanotube based potentiometric aptasensor, Angew. Chem. Int. Ed. 48 (2009) 7334-7373. https://doi.org/10.1002/anie.200902090

[21] N. Paniel, J. Baudart, A. Hayat, L. Barthelmebs, Aptasensor and genosensor methods for detection of microbes in real world samples, Methods 64 (2013) 229–240. https://doi.org/10.1016/j.ymeth.2013.07.001

[22] V. Pavlov, Y. Xiao, B. Shlyahovsky, I. Willner, Aptamer-functionalized Au nanoparticles for the amplified optical detection of thrombin, J. Am. Chem. Soc. 126 (2004) 11768-11769. https://doi.org/10.1021/ja046970u

[23] G. Bayramoglu, C. Ozalp, M. Oztekin, U. Guler, B. Salih, M.Y. Arica, Design of an aptamer-based magnetic adsorbent and biosensor systems for selective and sensitive separation and detection of thrombin, Talanta 191 (2019) 59-66. https://doi.org/10.1016/j.talanta.2018.08.048

[24] E. Sharon, X. Liu, R. Freeman, O. Yehezkeli, I. Willner, Label-Free Analysis of Thrombin or Hg2+ Ions by Nucleic Acid-Functionalized Graphene Oxide Matrices Assembled on Field-Effect Transistors, Electroanalysis 25 (2013) 851-856. https://doi.org/10.1002/elan.201200581

[25] Y. Guo, J. Zhang, W. Zhang, D. Hu, Green fluorescent carbon quantum dots functionalized with polyethyleneimine, and their application to aptamer-based determination of thrombin and ATP, Microchim. Acta 186 (2019) 717. https://doi.org/10.1007/s00604-019-3874-y

[26] N. Jiang, T. Zhu, Y. Hu, Competitive aptasensor with gold nanoparticle dimers and magnetite nanoparticles for SERS-based determination of thrombin, Microchim. Acta 186 (2019) 747. https://doi.org/10.1007/s00604-019-3787-9

[27] B. Zheng, S. Cheng, W. Liu, M.H.W. Lam, H. Liang, Small organic molecules detection based on aptamer-modified gold nanoparticles-enhanced quartz crystal microbalance with dissipation biosensor, Anal.Biochem. 438 (2013) 144–149. https://doi.org/10.1016/j.ab.2013.03.030

[28] J. Lao, L. Han, Z. Wu, X. Zhang, Y. Huang, Y. Tang, T. Guo, Gold Nanoparticle-Functionalized Surface Plasmon Resonance Optical Fiber Biosensor: In Situ Detection of Thrombin With 1 nM Detection Limit, J. Light. Technol. 37 (2019) 2748-2755.

[29] S.A. Kurseev, A.M. Solovjev, M.M. Neumann, A.V. Medvedko, I.Y. Sakharov, Chemiluminescent and Colorimetric Aptamer-Based Assays of Human α-Thrombin, Anal. Lett. 53 (2020) 140-151. https://doi.org/10.1080/00032719.2019.1640718

[30] X. Wang, F. Gao, Y. Gong, G. Liu, Y. Zhang, C. Ding, Electrochemical aptasensor based on conductive supramolecular polymer hydrogels for thrombin detection with high selectivity, Talanta 205 (2019) 120140. https://doi.org/10.1016/j.talanta.2019.120140

[31] S. Chen, P. Liu, K. Su, X. Li, Z. Qin, W. Xu, J. Chen, C. Li, J. Qiu, Electrochemical aptasensor for thrombin using co-catalysis of hemin/G-quadruplex DNAzyme and octahedral Cu_2O-Au nanocomposites for signal amplification, Biosens. Bioelectron. 99 (2018) 338-345. https://doi.org/10.1016/j.bios.2017.08.006

[32] B. Qin, K. Yang, Voltammetric aptasensor for thrombin by using a gold microelectrode modified with graphene oxide decorated with silver nanoparticles, Microchim. Acta 185 (2018), 407. https://doi.org/10.1007/s00604-018-2924-1

[33] Y. Wang, F. Wang, Z. Han, K. Huang, X. Wang, Z. Liu, S. Wang, Y. Lu, Construction of sandwiched self-powered biosensor based on smart nanostructure and capacitor: Toward multiple signal amplification for thrombin detection, Sens. Actuator B. 304(2020) 127418. https://doi.org/10.1016/j.snb.2019.127418

[34] Y.H. Wang, H. Xia, K.J. Huang, X. Wu, Y.Y. Ma, R. Deng, Y.F. Lu, Z.W. Han, Ultrasensitive determination of thrombin by using an electrode modified with WSe2 and gold nanoparticles, aptamer-thrombin-aptamer sandwiching, redox cycling, and signal enhancement by alkaline phosphatase, Microchim. Acta, 185 (2018) 502. https://doi.org/10.1007/s00604-018-3028-7

[35] H.L. Shuai, X. Wu, K.J. Huang, Molybdenum disulfide sphere-based electrochemical aptasensors for protein detection, J. Mater. Chem. B 5 (2017) 5362-5372. https://doi.org/10.1039/C7TB01276D

[36] Y. Niu, M. Chu, P. Xu, S. Meng, Q. Zhou, W. Zhao, B. Zhao, J. Shen, An aptasensor based on heparin-mimicking hyperbranched polyester with anti-biofouling interface for sensitive thrombin detection, Biosens. Bioelectron. 101 (2018) 174-180. https://doi.org/10.1007/s00604-018-2924-1

[37] Y. Ji, L. Zhang, L. Zhu, J. Lei, J. Wu, H. Ju, Binding-induced DNA walker for signal amplification in highly selective electrochemical detection of protein, Biosens. Bioelectron. 96 (2017) 201-205. https://doi.org/10.1016/j.bios.2017.05.008

[38] X. Li, L. Shen, D. Zhang, H. Qi, Q. Gao, F. Ma, C. Zhang, Electrochemical impedance spectroscopy for study of aptamer–thrombin interfacial interactions, Biosens. Bioelectron. 23 (2008) 1624-1630. https://doi.org/10.1016/j.bios.2008.01.029

[39] I. Isildak, F. Navaeipour, H. Afsharan, G.S. Kanberoglu, I. Agir, T. Ozer, N. Annabi, E.E. Totu, B. Khalilzadeh, Electrochemiluminescence methods using CdS quantum dots in aptamer-based thrombin biosensors: a comparative study, Microchimica Acta, 187 (2020) 25. https://doi.org/10.1007/s00604-019-3882-y

[40] H.R. Jamei, B. Rezaei, A.A. Ensafi, An ultrasensitive electrochemical anti-lysozyme aptasensor with biorecognition surface based on aptamer/amino-rGO/ionic liquid/amino-mesosilica nanoparticles, Colloid Surface B, 181 (2019) 16-24. https://doi.org/10.1016/j.colsurfb.2019.05.030

[41] F. Du, H. Zhang, X. Tan, C. Ai, M. Li, J. Yan, M. Liu, Y. Wu, D. Feng, S. Liu, H. Han, Nitrogen-doped graphene quantum dots doped silica nanoparticles as enhancers for electrochemiluminescence thrombin aptasensors based on 3D graphene, J. Solid State Chem. 23 (2019) 2579-2588. https://doi.org/10.1007/s10008-019-04352-z

[42] X. Wang, D. Sun, Y. Tong, Y. Zhong, Z. Chen, A voltammetric aptamer-based thrombin biosensor exploiting signal amplification via synergetic catalysis by DNAzyme and enzyme decorated AuPd nanoparticles on a poly (o-phenylenediamine) support, Microchim. Acta 184 (2017) 1791-1799. https://doi.org/10.1007/s00604-017-2160-0

[43] B. He, Sandwich electrochemical thrombin assay using a glassy carbon electrode modified with nitrogen-and sulfur-doped graphene oxide and gold nanoparticles, Microchim. Acta 185 (2018) 344. https://doi.org/10.1007/s00604-018-2872-9

[44] Y. Wang, Y. Zhang, T. Yan, D. Fan, B. Du, H. Ma, Q. Wei, Ultrasensitive electrochemical aptasensor for the detection of thrombin based on dual signal amplification strategy of Au/ GS and DNA-CoPd NPs conjugates, Biosens. Bioelectron. 80 (2016) 640-646. https://doi.org/10.1016/j.bios.2016.02.042

[45] Y. Li, Y. Li, N. Xu, J. Pan, T. Chen, Y. Chen, W. Gao, Dual-signal amplification strategy for electrochemiluminescence sandwich biosensor for detection of thrombin, Sens. Actuator B 240 (2017) 742-748. https://doi.org/10.1016/j.snb.2016.09.043

[46] B. Rezaei, H.R. Jamei, A.A. Ensafi, Lysozyme aptasensor based on a glassy carbon electrode modified with a nanocomposite consisting of multi-walled carbon nanotubes, poly (diallyl dimethyl ammonium chloride) and carbon quantum dots, Microchim. Acta 185 (2018) 180. https://doi.org/10.1007/s00604-017-2656-7

[47] Z. Su, X. Xu, H. Xu, Y. Zhang, C. Li, Y. Ma, D. Song, Q. Xie, Amperometric thrombin aptasensor using a glassy carbon electrode modified with polyaniline and multiwalled carbon nanotubes tethered with a thiolated aptamer, Microchim. Acta 184 (2017) 1677-1682. https://doi.org/10.1007/s00604-017-2164-9

[48] J. Han, Y. Zhuo, Y. Chai, R. Yuan, Y. Xiang, Q. Zhu, N. Liao, Multi-labeled functionalized C60 nanohybrid as tracing tag for ultrasensitive electrochemical aptasensing, Biosens. Bioelectron. 46 (2013) 74-79. https://doi.org/10.1016/j.bios.2013.02.020

[49] L. Bai, Y. Chen, Y. Bai, Y. Chen, J. Zhou, A. Huang, Fullerene-doped polyaniline as new redox nanoprobe and catalyst in electrochemical aptasensor for ultrasensitive detection of Mycobacterium tuberculosis MPT64 antigen in human serum, Biomaterials 133 (2017) 11-19. https://doi.org/10.1016/j.biomaterials.2017.04.010

[50] Y. Duan, Y. Yang, J. Wang, H. Li, K. Liu, A facile one-pot synthesis of polyethyleneimine functionalized graphene for the highly-sensitive and selective electrochemical impedance aptasensing of kanamycin in serum, Anal. Methods 12 (2020) 132-140. https://doi.org/10.1039/C9AY02120E

[51] H. Wu, H. Shi, H. Zhang, X. Wang, Y. Yang, C. Yu, C. Hao, J. Du, H. Hu, S. Yang, Prostate stem cell antigen antibody-conjugated multiwalled carbon nanotubes for targeted ultrasound imaging and drug delivery, Biomaterials 35 (2014) 5369-5380. https://doi.org/10.1016/j.biomaterials.2014.03.038

[52] L. Ma, L. Bai, M. Zhao, J. Zhou, Y. Chen, Z. Mu, An electrochemical aptasensor for highly sensitive detection of zearalenone based on PEI-MoS2-MWCNTs nanocomposite for signal enhancement, Anal. Chim. Acta 1060 (2019) 71-78. https://doi.org/10.1016/j.aca.2019.02.012

[53] C. Wang, J. Zhou, G. Ran, F. Li, Z. Zhong, Q. Song, Q. Dong, Bi-functional fluorescent polymer dots: a one-step synthesis via controlled hydrothermal treatment and application as probes for the detection of temperature and Fe^{3+}, J. Mater. Chem. C 5 (2017) 434-443. https://doi.org/10.1039/C6TC04286D

[54] J. Xia, Y.T. Zhuang, Y.L. Yu, J.H. Wang, Highly fluorescent carbon polymer dots prepared at room temperature, and their application as a fluorescent probe for determination and intracellular imaging of ferric ion, Microchim. Acta 184 (2017) 1109-1116. https://doi.org/10.1007/s00604-017-2104-8

[55] C. Piaopiao, X. Yichen, C. Xiaoxiao, Z. Shan, L. Yang, H. Chaobiao, A "Signal On" Photoelectrochemical Aptasensor For Tetracycline Detection Based On Semiconductor Polymer Quantum Dots, J. Electrochem. Soc. 167 (2020) 067516.

[56] F. Sun, Z. Wang, Y. Feng, Y. Cheng, H. Ju, Y. Quan, Electrochemiluminescent resonance energy transfer of polymer dots for aptasensing, Biosens. Bioelectron.100 (2018) 28-34. https://doi.org/10.1016/j.bios.2017.08.047

[57] S. Yang, Y. Teng, Q. Cao, C. Bai, Z. Fang, W. Xu, Electrochemical sensor based on molecularly imprinted polymer-aptamer hybrid receptor for voltammetric detection of thrombin, J. Electrochem. Soc. 166 (2019) 23.

[58] K.N. Semenov, E.V. Andrusenko, N.A. Charykov, E.V. Litasova, G.G. Panova, A.V. Penkova, I.V. Murin, L.B. Piotrovskiy, Carboxylated fullerenes: Physico-chemical properties and potential applications, Prog Solid State Ch. 47 (2017) 19-36. https://doi.org/10.1016/j.progsolidstchem.2017.09.001

[59] A.A. Ensafi, H.R. Jamei, E. Heydari-Bafrooei, B. Rezaei, Development of a voltammetric procedure based on DNA interaction for sensitive monitoring of chrysoidine, a banned dye, in foods and textile effluents, Sens. Actuator B. 202 (2014) 224-231. https://doi.org/10.1016/j.snb.2014.05.001

[60] A.E. Radi, J.L. Acero Sánchez, E. Baldrich, C.K. O'Sullivan, Reagentless, reusable, ultrasensitive electrochemical molecular beacon aptasensor, J. Am. Chem. Soc. 128 (2006) 117-124. https://doi.org/10.1021/ja053121d

[61] Q. Chen, H. Chen, Y. Zhao, F. Zhang, F. Yang, J. Tang, P. He, A label-free electrochemiluminescence aptasensor for thrombin detection based on host–guest recognition between tris (bipyridine) ruthenium (II)-β-cyclodextrin and aptamer, Biosens. Bioelectron. 54 (2014) 547-552. https://doi.org/10.1016/j.bios.2013.11.028

[62] Y. Wu, L. Zou, S. Lei, Q. Yu, B. Ye, Highly sensitive electrochemical thrombin aptasensor based on peptide-enhanced electrocatalysis of hemin/G-quadruplex and nanocomposite as nanocarrier, Biosens. Bioelectron. 97 (2017) 317-324. https://doi.org/10.1016/j.bios.2017.06.023

[63] H. Wu, M. Li, Z. Wang, H. Yu, J. Han, G. Xie, S. Chen, Highly stable Ni-MOF comprising triphenylamine moieties as a high-performance redox indicator for sensitive aptasensor construction, Anal. Chim. Acta 1049 (2019) 74-81. https://doi.org/10.1016/j.aca.2018.10.022

[64] Q. Xu, G. Wang, M. Zhang, G. Xu, J. Lin, X. Luo, Aptamer based label free thrombin assay based on the use of silver nanoparticles incorporated into self-polymerized dopamine, Microchim. Acta, 185 (2018) 253. https://doi.org/10.1007/s00604-018-2787-5

[65] F. Gao, L. Du, Y. Zhang, F. Zhou, D. Tang, A sensitive sandwich-type electrochemical aptasensor for thrombin detection based on platinum nanoparticles decorated carbon nanocages as signal labels, Biosens. Bioelectron. 86 (2016) 185-193. https://doi.org/10.1016/j.bios.2016.06.055

[66] W. Xu, H. Yi, Y. Yuan, P. Jing, Y. Chai, R. Yuan, G.S. Wilson, An electrochemical aptasensor for thrombin using synergetic catalysis of enzyme and porous Au@ Pd core–shell nanostructures for signal amplification, Biosens. Bioelectron. 64 (2015) 423-428. https://doi.org/10.1016/j.bios.2014.08.091

Figure Captions

Fig. 1 Schematic of step-wise preparation electrochemical aptasensor and C_{60}/MWCNTs-PEI/PQdot.

Fig. 2 TEM and FE-SEM images (A-H) of unmodified SPCE (A), MWCNTs (B and C), fullerene C_{60} (D), Prepared C_{60}/MWCNTs (E), C_{60}/MWCNTs-PEI (F and G), C_{60}/MWCNTs-PEI/PQdot nanocomposite (H). CV and DPV voltammograms (I and J) and EIS Nyquist plots (K) of (a) unmodified SPCE, and modified SPCE with (b) MWCNTs, (c) C_{60}/MWCNTs, (d) C_{60}/MWCNTs-PEI, and (e) C_{60}/MWCNTs -PEI/PQdot nanocomposites in a solution containing 2.5 mmol L^{-1} $[Fe(CN)6]^{3-/4-}$ (1:1) mixture and 0.1 mol L^{-1} KCl (in TE buffer with pH=7.4).

Fig. 3 (A, C and E) DPV voltammograms of (a) bare SPCE, (b) modified SPCE of with different nanocomposites, (c) immobilized aptamer on the modified electrodes with different nanocomposites, and (d) aptamer fitted to thrombin (0.005 nmol L^{-1}). (B, D and F) I (μA) variation for each step in the detection of thrombin was measured via prepared aptasensor, in which different nanocomposites was applied as sensitive layers. Electrode modification and aptosensor development were performed with C_{60}/MWCNTs (A and B), C_{60}/MWCNTs-PEI (C

and D), C_{60}/MWCNTs-PEI/PQdot (E and F) nanocomposites. DPV voltammograms acquired in a solution containing 2.5 mmol L^{-1} $[Fe(CN)6]^{3-/4-}$ (1:1) mixture and 0.1 mol L^{-1} KCl (in TE buffer with pH=7.4).

Fig. 4 (A) DPV voltammograms of thrombin aptasensor-based SPCE/C_{60}/MWCNTs-PEI/PQdot for different concentrations of thrombin within 50 fmol L^{-1} – 20 nmol L^{-1}, (B) calibration curve for ΔI (n=3) vs. ($C_{Thrombin}$, nmol L^{-1}), (C) ΔI vs. log ($C_{Thrombin}$, nmol L^{-1}), and (D) ΔI_p of the thrombin aptasensor-based SPCE/C_{60}/MWCNTs-PEI/PQdot relating to (a) 0.0005 nmol L^{-1} thrombin, mixtures of 0.0005 nmol L^{-1} Thrombin with (b) 0.01 nmol L^{-1} Lys, (c) 0.05 nmol L^{-1} BSA, (d) 0.05 nmol L^{-1} IgG, and (e) 0.03 nmol L^{-1} BHb, respectively, (n=4).

Table Captions

Table 1. Comparison of proposed SPCE/C_{60}/MWCNTs-PEI/PQdot/GLA/APT aptasensor with other electrochemical aptamers that have been proposed in recent years for thrombin protein analysis.

Table 2. Recovery measurements of thrombin protein for real sample analysis in the presence of proposed SPCE/C_{60}/MWCNTs-PEI/PQdot/GLA/APT aptasensor.

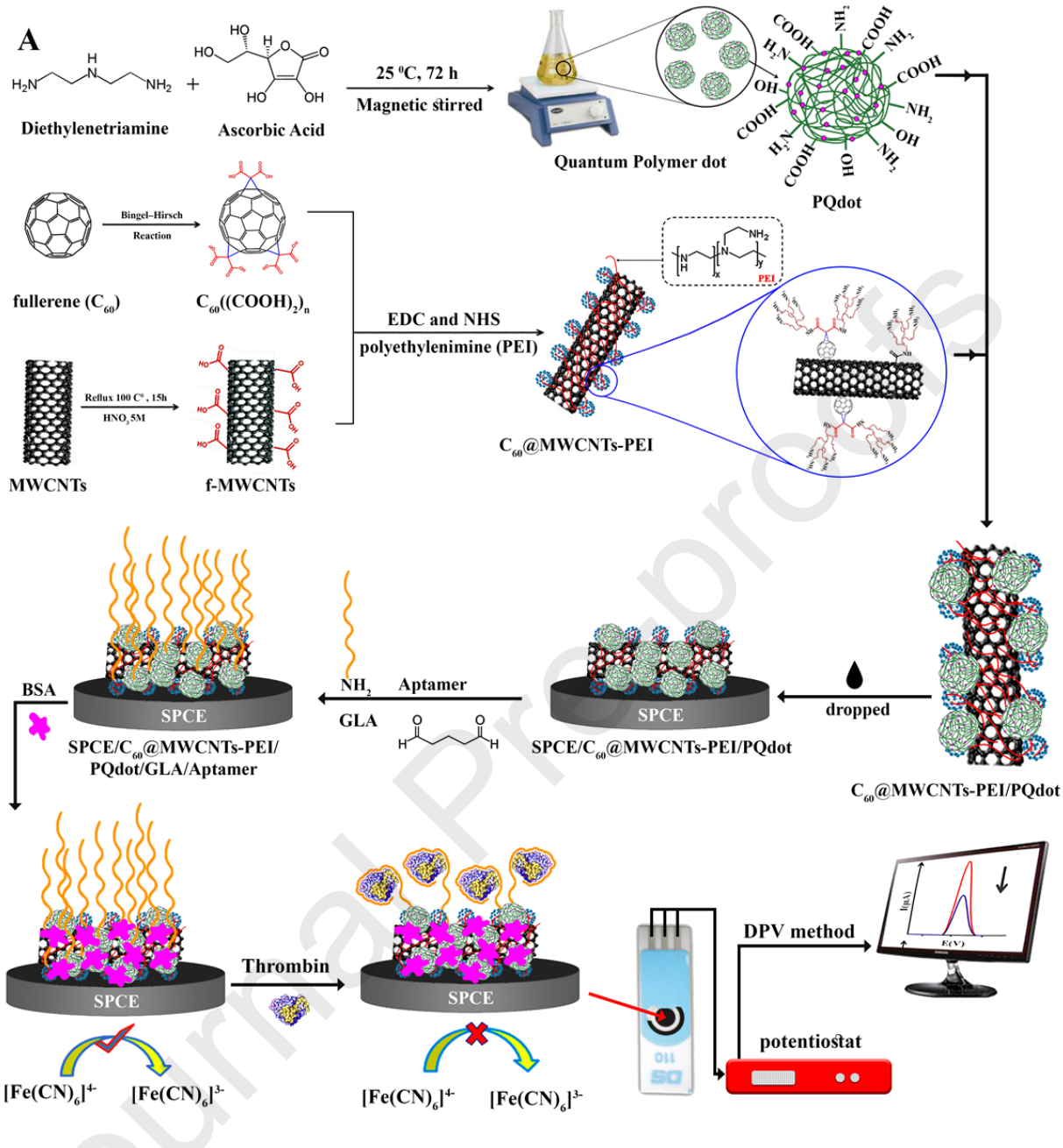
A
Diethylenetriamine
Ascorbic Acid
25 °C, 72 h
Magnetic stirred
Quantum Polymer dot
PQdot
Bingel–Hirsch Reaction
fullerene (C_{60})
$C_{60}((COOH)_2)_n$
Reflux 100 C°, 15h
HNO_3 5M
MWCNTs
f-MWCNTs
EDC and NHS
polyethylenimine (PEI)
PEI
C_{60}@MWCNTs-PEI
dropped
C_{60}@MWCNTs-PEI/PQdot
SPCE
SPCE/C_{60}@MWCNTs-PEI/PQdot
NH_2 Aptamer
GLA
BSA
SPCE/C_{60}@MWCNTs-PEI/ PQdot/GLA/Aptamer
Thrombin
DPV method
potentiostat
$[Fe(CN)_6]^{4-}$
$[Fe(CN)_6]^{3-}$

Fig. 1

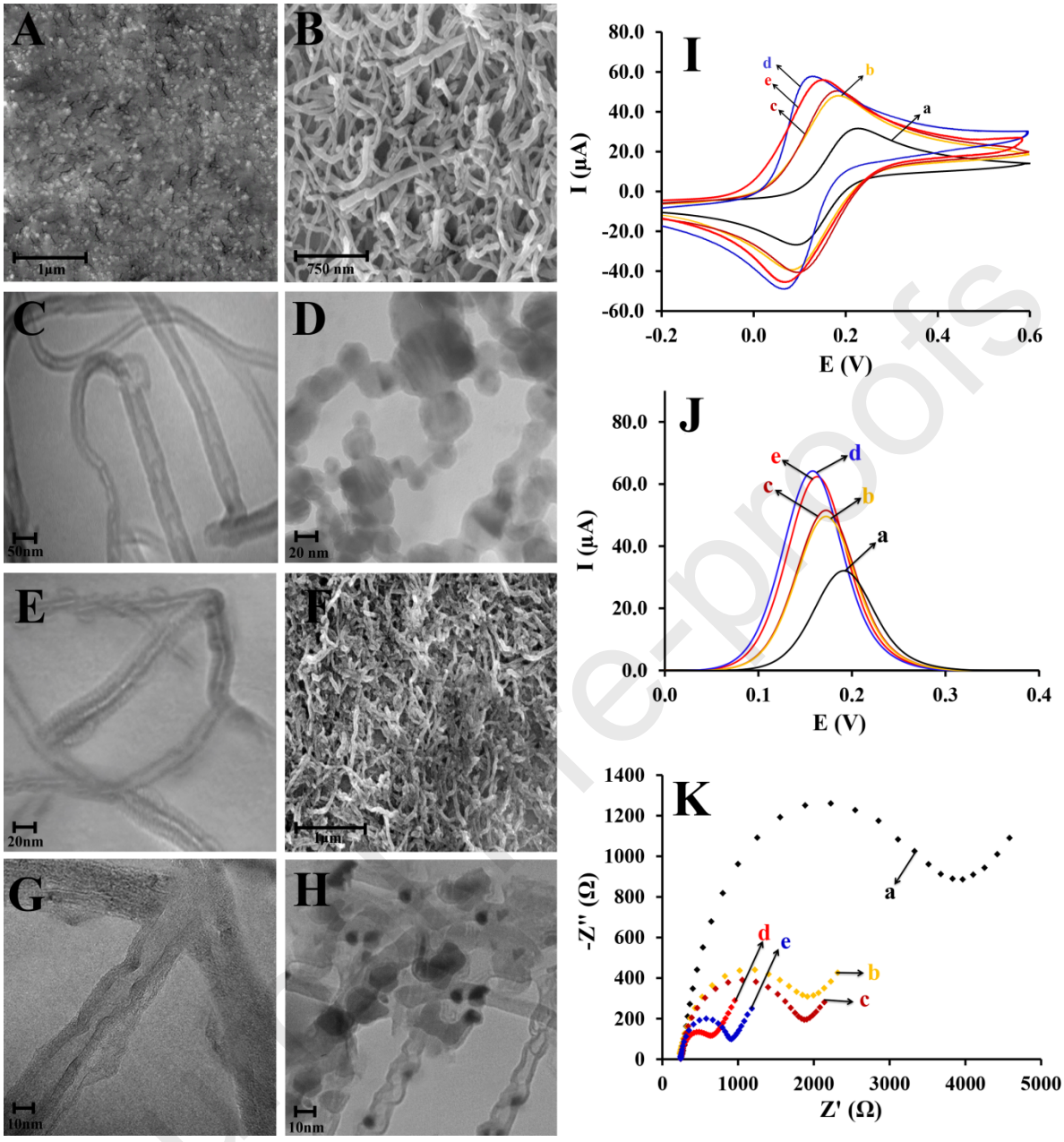
A
1μm
B
750 nm
C
50nm
D
20 nm
E
20nm
F
1μm
G
10nm
H
10nm
I
I (μA)
E (V)
a
b
c
d
e
J
I (μA)
E (V)
K
-Z'' (Ω)
Z' (Ω)

Fig. 2

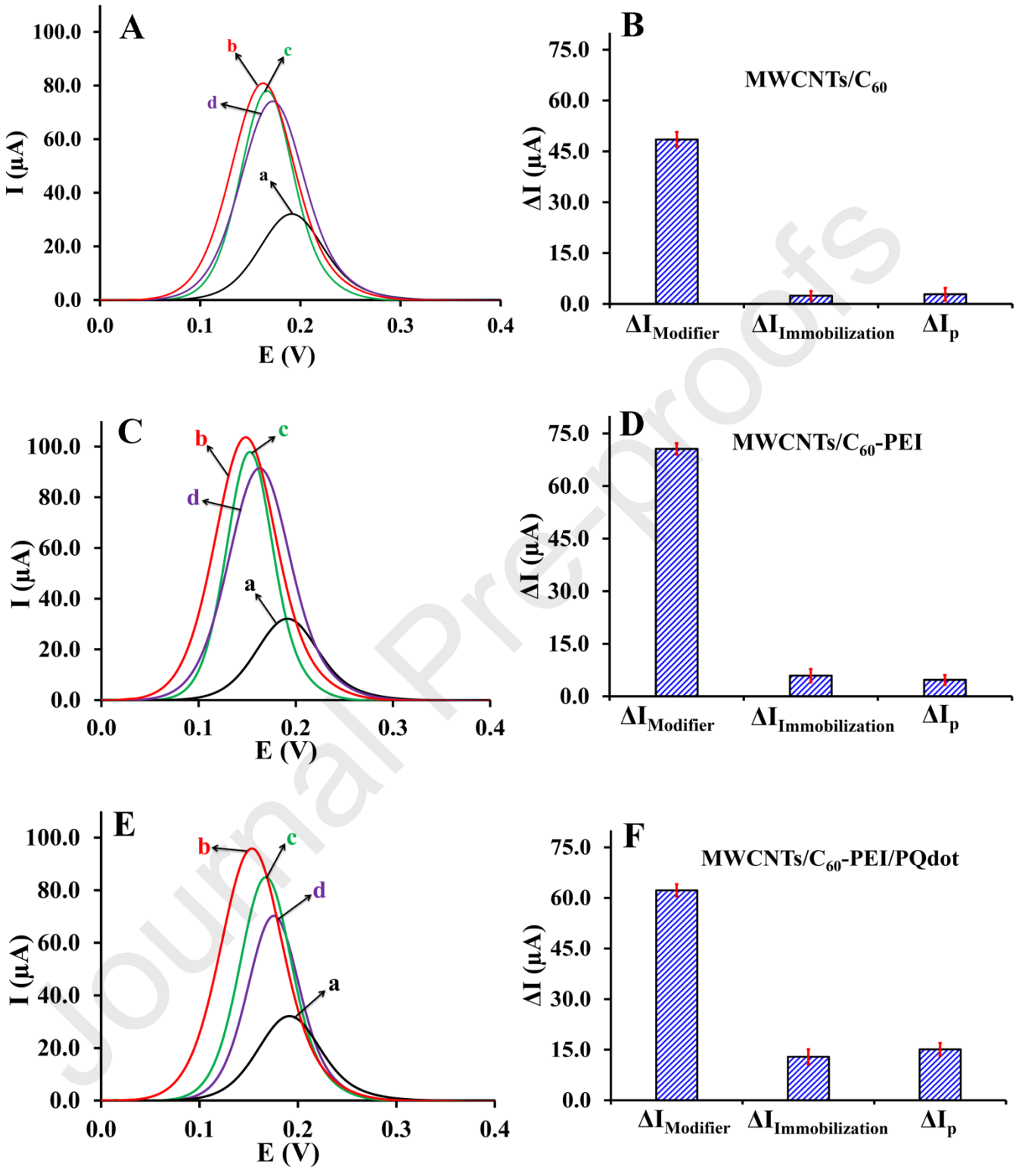
A
B
C
D
E
F
I (μA)
E (V)
ΔI (μA)
MWCNTs/C60
MWCNTs/C60-PEI
MWCNTs/C60-PEI/PQdot
ΔIModifier
ΔIImmobilization
ΔIp
a
b
c
d

Fig. 3

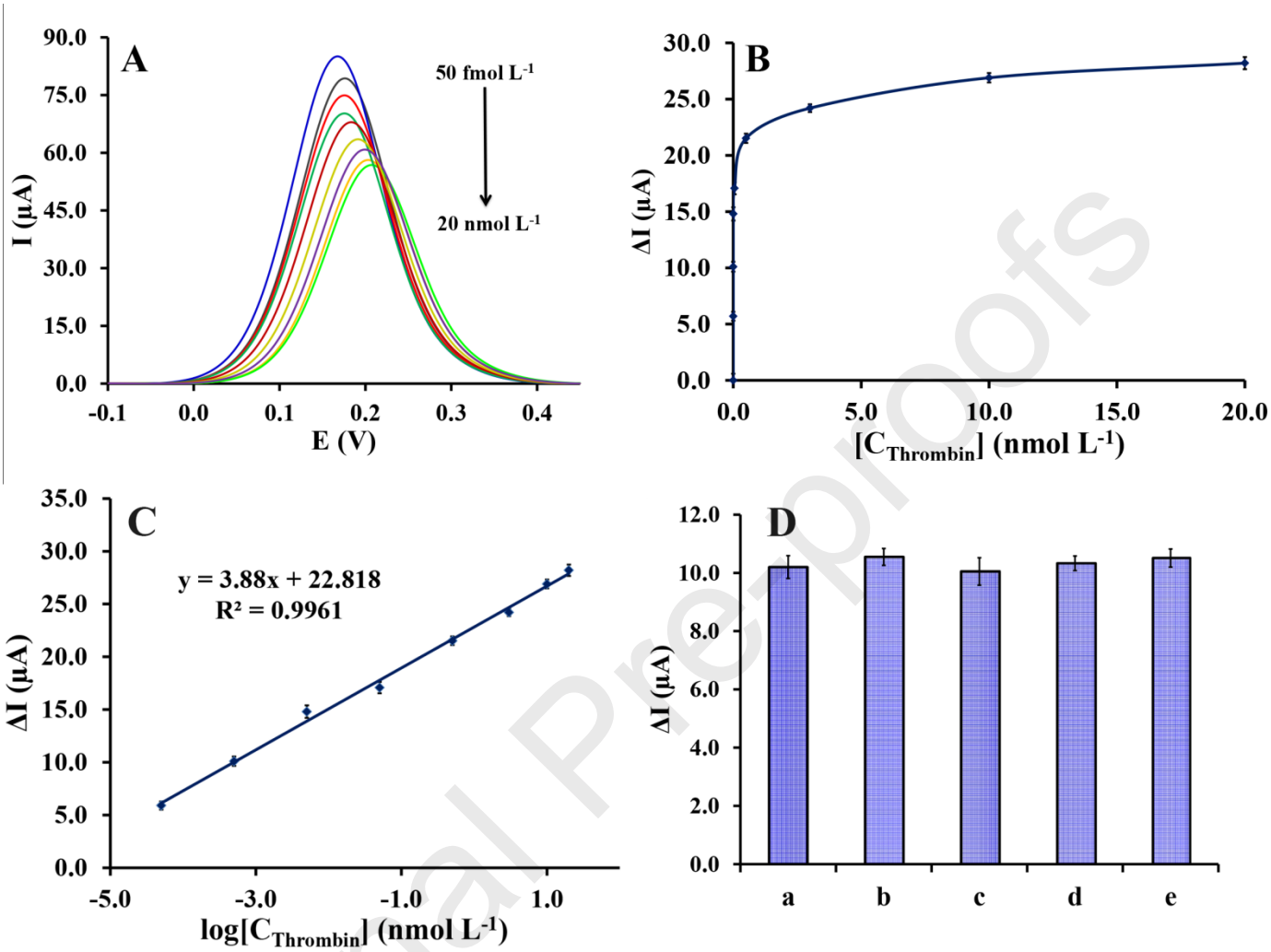

Fig. 4

Table 1

Method	Strategy	Linear Range	LOD	RSD%	Ref.
DPV	Fc-TBA/Au /Aptamer	5.0 nM - 35 nM	0.5 nM	3.8% to 10.0%	[60]
ECL	Tri(bpyRu)-β-D/Aptamer	1.0 pM - 10 nM	0.1 pM	-	[61]
ECL	3D graphene/Ru-PtNPs/cDNA/BSA /NGQDs/SiO_2/TBA	2.0 pM - 50 nM	23.1 fM	3.02%	[41]
DPV	TBA/HBPE-SO_3/Au/MPTMS/GCE	2.70 pM - 27.0μM	0.031 pM	3.68%	[36]
DPV	AuNPs/N-GO/GCE	0.0001–100 pM	0.027 fM	4.2%	[35]
ACV	Binding-induced DNA walker-assisted	10 pM - 100 nM	2.5 pM	3.5%	[37]
DPV	Electrocatalysis of hemin/ G-quadruplex	0.05 pM - 60.0nM	15 fM	4.68%	[62]
DPV	Conductive supramolecular hydrogels	1 pM - 10 nM	0.64 pM	2.3% to 4.5%	[30]
Chronoamperometry	Cu_2O-Au/ Aptamer	100 fM - 20 nM	23fM	0.49% to 1.29%	[31]
DPV	AP II bioconjugate/Tb/BSA/API/DpAu/GCE	0.05 pM - 50 nM	0.016 pM	4.63%	[63]
DPV	Tetrahedral DNA probe coupling with hybridization chain	0.10 pM -10 nM	11.6 fM	3.9%	[2]
DPV	TiO_2-MWCNT/CHIT-SB/ Aptamer	0.05 nM -10 nM	10 fM	3.6%	[6]
SWV	TBA2-thrombin-TBA1-AgNP-GO	0.05 nM -5 nM	0.03 nM	3.7%	[32]
DPV	Gquadruplex/hemin/HRP/AuPd/poly(o-phenylenediamine)	100 fM - 20 nM	20 fM	4.5%	[42]
EIS	TBA/HT/GNPs/GCE/ Aptamer	0.12 nM - 60 nM	2.0 nM	4.5%	[38]
DPV	Pt NPs /gold GCE	0.05–20000 pM	0.01 pM	3.2%	[65]
DPV	TTA-PANI-MWCNTs/GCE/ Aptamer	0.001 nM - 10 nM	0.5 pM	4.3%	[47]
DPV	AuNP-SN-GO/GC/ Aptamer	100 fM -10 nM	25 fM	2.4%	[43]
EIS	PDA/AgNP/Aptamer	0.1 pM - 5.0 nM	36 fM	4.7%	[64]
DPV	MWCNT/MnO2/Pt NPs/Tb	1pM to 30nM	0.040 pM	5.6%	[66]
ECL	AuNP/GO/Aptamer	10 pM -10 nM	6.3 pM	2.7-3.1%	[45]
Amperometry	Au/GS and DNA-CoPd NPs	0.3 pM -54 pM	0.14 pM	4.1%	[44]
DPV	C60/MWCNTs-PEI/CS/PQdot/GLA/APT	50 fM -20 nM	6 fM	3.6%	**This work**

Table 2

Samples	spiked Thrombin (pM)	Found (pM)	RSD (%)	Recovery (%)
Serum 1	0.50	0.48 ± 0.02	4.2	96.0
	5.00	4.90 ± 0.19	3.9	98.0
	50.00	51.04 ± 1.73	3.4	102.3
Serum 2	0.50	0.52 ± 0.03	5.8	104
	5.00	5.21 ± 0.25	4.8	104.2
	50.00	49.72 ± 1.95	3.9	99.4
Serum 3	0.50	0.51 ± 0.02	5.9	102.0
	5.00	4.77 ± 0.21	4.4	95.4
	50.00	48.69 ± 1.84	3.8	97.4

Graphical abstract

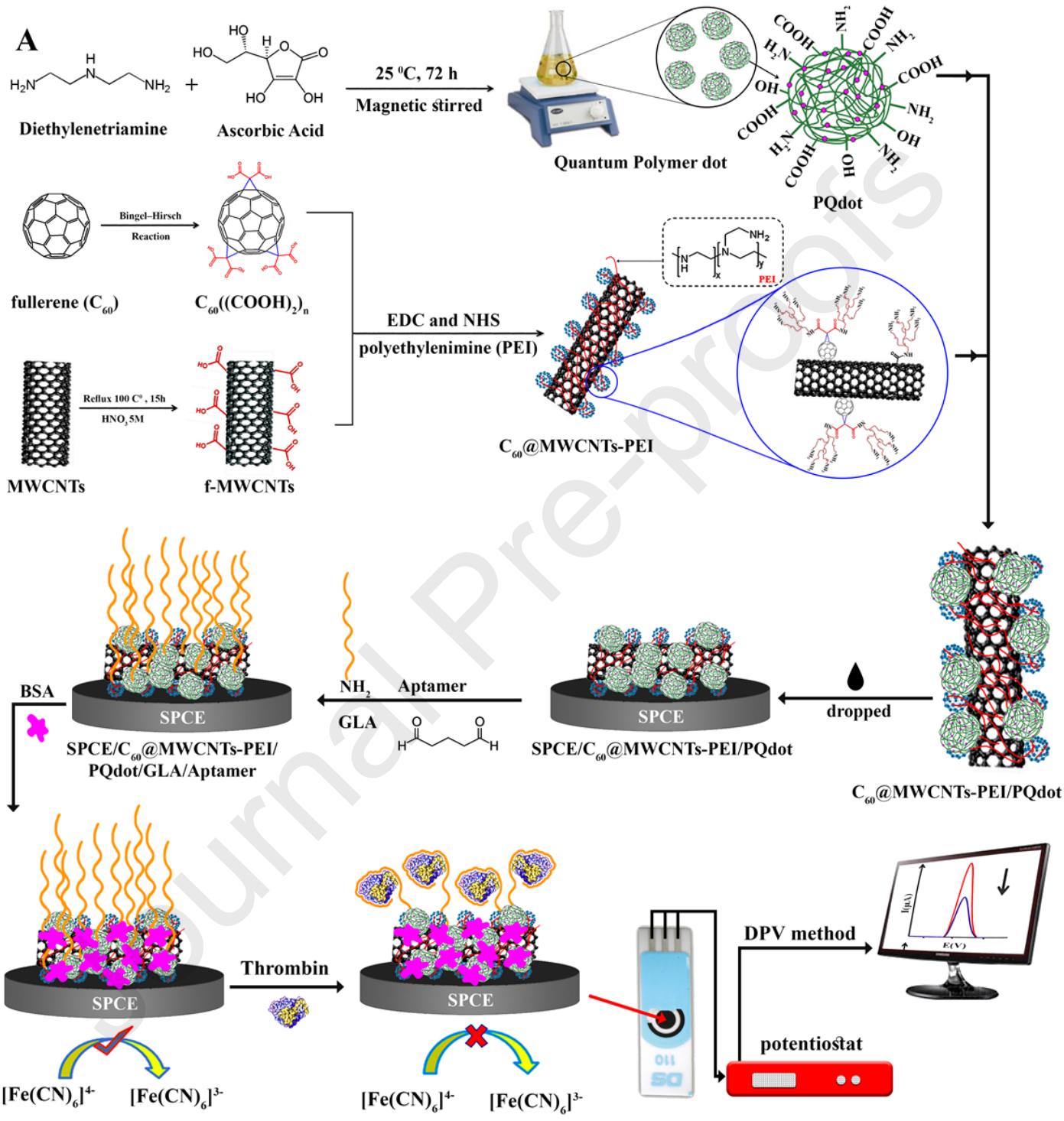

Highlights:

- C_{60}/MWCNTs-PEI/PQdot nanocomposite was used to develop an electrochemical aptasensor for thrombin protein detection
- The synthesized polymer quantum dots and C_{60}/MWCNTs-PEI resulted in increase in electrochemical signal, therefore increasing the sensitivity of developed electrochemical aptasensor.
- C_{60}/MWCNTs-PEI/PQdot provides a suitable base for covalent stabilization of aptamers.
- The proposed aptasensor displayed low LOD of 6 fmol L^{-1} for thrombin protein detection.

Declaration of interests

☒ The authors declare that they have no known competing financial interests or personal relationships that could have appeared to influence the work reported in this paper.

☐The authors declare the following financial interests/personal relationships which may be considered as potential competing interests: